## Graphical abstract

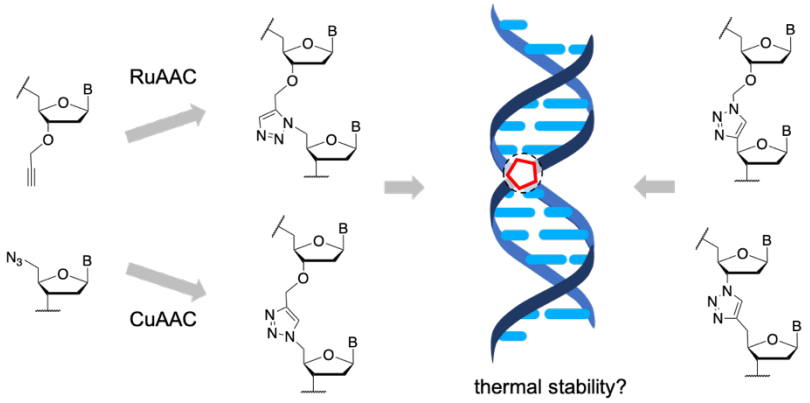


# Searching for the ideal triazole: Investigating the 1,5-triazole as a charge neutral DNA backbone mimic

Ysobel R. Baker[a], Diallo Traoré[a †], Przemyslaw Wanat[a, b], Agnès Tyburn[a §], Afaf H. El-Sagheer[a,c], Tom Brown[a]*

[a]Chemistry Research Laboratory, University of Oxford, 12 Mansfield Road, Oxford, OX1 3TA, UK
[b]Faculty of Physics, University of Warsaw; L. Pasteura 5, 02-093 Warsaw, Poland
[c]Chemistry Branch, Department of Science and Mathematics, Faculty of Petroleum and Mining Engineering, Suez University, Suez 43721, Egypt

*email: tom.brown@chem.ox.ac.uk

## Abstract

A novel triazole linkage that mimics the phosphodiester backbone in DNA was designed, synthesised and evaluated. Unlike previous work which utilised copper to form a 1,4 triazole linkage in the DNA backbone, a ruthenium catalyst was used to yield a 1,5 triazole. The artificial linkage was incorporated into a DNA backbone *via* a phosphoramidite building block using solid phase synthesis. The biophysical properties of DNA with a 1,5 triazole linkage in the backbone were evaluated by UV melting and circular dichroism and compared to DNA modified with previously reported 1,4 triazole linkages of various lengths.

## Introduction

Antisense oligonucleotides (ASOs) are synthetic analogues of nucleic acids which target mRNA, modulating gene expression and therefore protein production.[1] They are rapidly becoming important therapeutic agents for treating challenging diseases. Unlike small molecules drugs, ASOs are informational in nature where the target is defined by the sequence of bases.[2] This key advantage means that an ASO can be rationally designed to have high specificity against any genomic target, including hard to treat cancers[3] and rare diseases.[4] Modification of the chemical architecture of ASOs is necessary for clinical utility and stability *in vivo* and many different chemistries have been developed to improve the drug-like properties of oligonucleotides.[2, 5-8] Despite this, ASOs are only just reaching

Authors current addresses:
† Faculty of Fundamental and Biological Sciences, Université Paris Descartes, 45 rue des Saints Pères 75006, Paris France
§ Illumina, 19 Granta park, Cambridge, CB21 6DF

the clinic[9-13] and several obstacles remain; these include inefficient intracellular delivery to targeted tissues[14] and unknown long-term safety and off targeting effects.[2]

Modifications can be made to the sugar, phosphodiester backbone, nucleobases or the terminus of nucleic acids to improve the drug-like properties of ASOs.[2] Recently, our group and others have been interested in using copper catalysed alkyne-azide cycloaddition (CuAAC) click chemistry to substitute the phosphate backbone of DNA with triazole linkages,[15-22] examples are shown in Figure 1. These linkages increase the stability of oligonucleotides towards nuclease degradation and reduce their overall anionic charge, a factor that has been suggested to aid cellular uptake, making the triazole linkage (TL) an interesting candidate for ASOs.

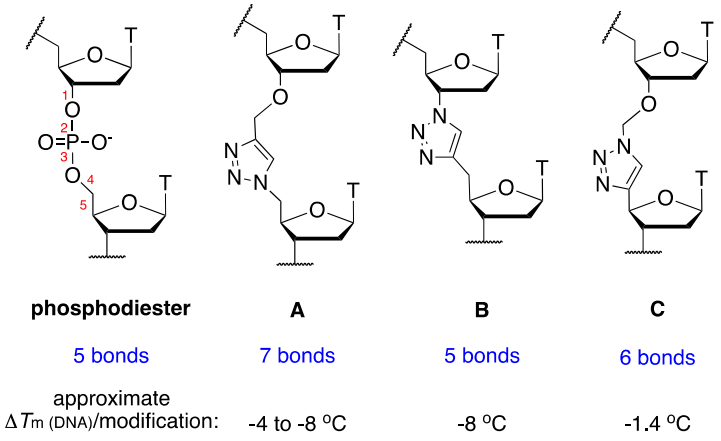


**Figure 1**. Examples of 1,4 triazole linkages, their inter-sugar spacing (shown in blue) counted as the number of bonds (shown in red), and their influence on duplex stability. A) Biocompatible triazole first reported by Zerrouki et al;[18-20] B) Triazole reported by Isobe et al;[21] C) Triazole reported by Varizhuk et al.[22]

Despite these advantages, oligonucleotides with TLs suffer from reduced binding affinity to complementary target nucleic acids, limiting their use in applications such as antisense, where high duplex thermal stability and good mismatch discrimination are necessary. Whilst TL **A** with 7 bond spacing can be correctly read by both DNA and RNA polymerases,[19, 20, 23] it reduces oligonucleotide binding affinity towards target DNA and RNA ($\Delta T_m \approx$ -4 to -8 °C/modification when compared with an unmodified duplex).[24, 25] The shorter 5 bond TL **B** has been used to construct a fully triazole-modified DNA analogue which formed a stable duplex with DNA ($\Delta T_m \approx$ +4 °C/modification);[21] however, when TL **B** was later tested as an isolated modification within a phosphodiester backbone environment the resulting duplexes were also found to be unstable ($\Delta T_m \approx$ -8 °C/modification).[26] To the best of our knowledge, TL **C** with 6 bonds is the least destabilising TL when studied in a DNA:DNA duplex (average $\Delta T_m \approx$ -1.4 °C/modification),[22] but its affinity towards RNA has not yet been reported.

Several strategies have been developed to improve target affinity of triazole containing oligonucleotides, including flanking the triazole with LNA[27-29] and adding a G-clamp to the neighbouring nucleobase.[25] Whilst these are valid approaches, it is clear that the precise nature of the TL can have a significant effect on the hybridisation properties of the parent oligonucleotides and that optimization of the linkage should be considered carefully.

Knowing that changing the catalyst in the alkyne-azide cycloaddition reaction from Cu(I) to ruthenium Ru(II) results in a 1,5 rather than a 1,4-triazole piqued our curiosity towards the 1,5 TL **D** as a phosphodiester mimic (Figure 2).[30, 31] When used in the context of the DNA backbone, a 1,5 triazole would produce a linkage that is one bond shorter than the corresponding 1,4 triazole, with the substituents spaced at 3.2 Å rather than 4.9 Å (Figure 2).[32] The 1,5 TL **D** would have the same bond

spacing (6) as the most thermally stable 1,4 TL **C**, and we hypothesized that TL **D** would be readily accessible from the alkyne and azide precursors used to synthesise the 7 bond 1,4 TL **A** (Figure 1). We were further encouraged to pursue a 1,5 TL by awareness of the previously reported 1,5 TL **E**.[33] Both the 1,5 TL **E** and the 1,4 TL **B** have a 5 bond inter-sugar spacing; however, TL **E** is reported to be considerably less destabilising ($\Delta T_m$ between -2.3 and -6.1 °C/modification against RNA).

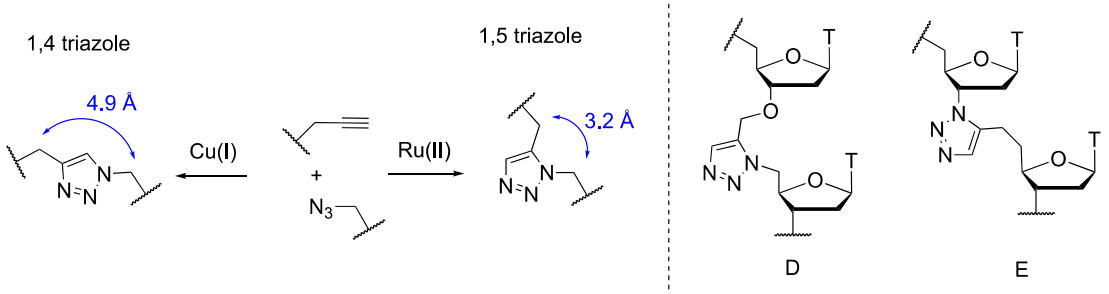


**Figure 2**. The 1,5 triazole linkage and spacing of the methylene substituents.[32] Left) The choice of catalyst determines the product of the 1,3 dipolar alkyne-azide cycloaddition; Right) TL **D** investigated in this study and TL **E** prepared previously using a thermal cycloaddition of a 2-oxoalkylidene triphenylphosphorane and an azide.[34]

Consequently, we decided to evaluate the 6 bond 1,5 TL **D** as a phosphodiester mimic. We included the 1,4 triazole linkages **A**-**C** in this study as, whilst all have been evaluated in DNA:DNA duplexes, the variability of the sequences and precise conditions used in duplex melting studies prevent a direct comparison between the modifications. In addition, the 1,4 TLs **B** and **C** have not previously been studied in duplexes against complementary RNA, which would be the target of an ASO, and it is important to compare their RNA-binding properties when developing new ASO candidates.

## 1. Results and discussion

### *1.1. Synthesis of dinucleoside phosphoramidites*

We first prepared the required 5'- O -DMT-protected phosphoramidite building blocks with 1,4 triazole linkages **A**-**C** and 1,5 TL **D** between two thymidine nucleosides for use in solid phase oligonucleotide synthesis (Figure 3). Alkyne **1**[35] and azide **2**[36] were each synthesised in a single step from commercially available 4,4'-dimethoxytrityl thymidine and thymidine respectively. Initial attempts at coupling alkyne **1** and azide **2** using 20 mol% Cp*RuCl($PPh_3$)$_2$ as a catalyst in toluene were low yielding (5-10%). We suspected that this was due to the limited solubility of the intermediate and repeated the reaction in different aprotic solvents (tetrahydrofuran, dichloroethane and dioxane). Complete conversion of starting material to product took 4 h in dioxane, 8 h in tetrahydrofuran and did not go to completion in dichloroethane or toluene. Using dioxane as a solvent the T-T dimer **3** was obtained in 95% yield. Phosphitylation of alcohol **3** proceeded smoothly to give the 1,5 TL **D** phosphoramidite building block **4** in 74% yield. In addition, we prepared phosphoramidites **5**,[37] **6**[26] and **7**[22] according to literature procedures.

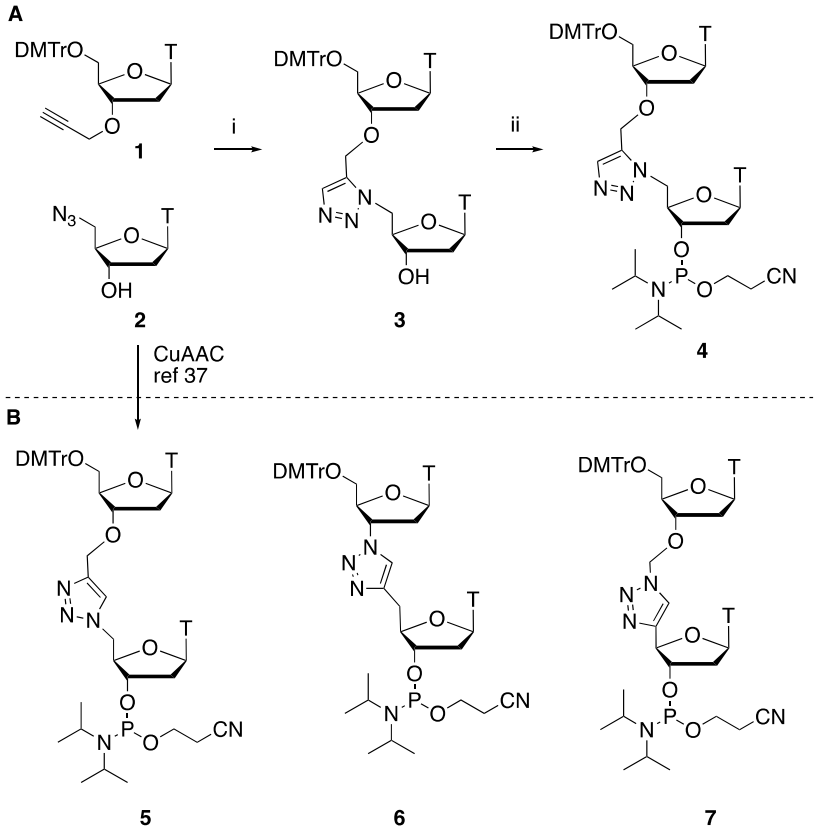


**Figure 3**. Phosphoramidite building blocks used in this study. A) Synthesis of the 1,5 TL **D** building block **4**. *Reagents and conditions:* i) Cp*Ru(PPh$_3$)$_2$Cl, dioxane, 80 °C, 4 h, 95%; ii) 2-cyanoethyl *N*,*N*-diisopropylchlorophosphoramidite, *N*,*N*-diisopropylethylamine (DIPEA), $CH_2Cl_2$, rt, 74%; B) Phosphoramidites **5**,[37] **6**[26] and **7**[22] were synthesised as previously described to investigate the 1,4 TLs **A**-**C** respectively. T = thymine, DMTr = 4,4'-dimethoxytrityl.

*1.2. DNA and RNA duplex stability*

Phosphoramidites **4**-**7** were used to synthesise the oligonucleotides (ONs) in Table 1 that were required for UV melting studies. Standard solid-phase protocols were used, increasing the coupling time for the modified phosphoramidites to 10 min. No decrease in coupling efficiency was observed when incorporating these dimer phosphoramidites.

The hybridization properties of DNA modified with the different triazole linkages were compared. UV melting was used to determine the melting temperature ($T_m$) of ON 1-4 against DNA (Figure 4) and RNA (Figure 5), and the $T_m$s are listed in Table 1. We have previously used ON 1 in NMR studies to explain the biocompatibility of the DNA triazole linkage and the $T_m$s of the DNA:DNA[24] and DNA:RNA[37] duplexes have been reported, providing a benchmark for this work.

In agreement with the previous studies discussed earlier, DNA containing 1,4 TLs **A**-**C** all form less stable duplexes with DNA than that of the unmodified DNA control (Figure 4). The short 5 bond 1,4 TL **B** was most destabilising ($\Delta T_m$ = -11.2 °C). 1,4 TL **A** with 7 bonds performed better than the shorter TL **B**, but was still strongly destabilising ($\Delta T_m$ = -7.4 °C). The 1,4 TL **C** ($\Delta T_m$ = -3.2 °C) and 1,5 TL **D** ($\Delta T_m$ = -2.9 °C) with 6 bonds were the least destabilising, reducing the duplex stability to a similar degree. The circular dichroism (CD) spectra of these duplexes suggest that all TL modified DNA:DNA duplexes adopt the B form (Figure 4).

**Table 1.** Thermal melting ($T_m$) data for triazole DNA:DNA and triazole DNA:RNA duplexes

| ON | Triazole linkage[a] | Linkage length/bonds | DNA target[b] $T_m$[d] ($\Delta T_m$[e]) /°C | RNA target[c] $T_m$[d] ($\Delta T_m$[e]) /°C |
|---|---|---|---|---|
| 1 | **A** (1,4) | 7 | 54.5 (-7.4) | 53.3 (-5.3) |
| 2 | **B** (1,4) | 5 | 50.7 (-11.2) | 45.0 (-13.6) |
| 3 | **C** (1,4) | 6 | 58.7 (-3.2) | 57.8 (-0.8) |
| 4 | **D** (1,5) | 6 | 59.0 (-2.9) | 55.3 (-3.3) |
| 5 | Phosphodiester | 5 | 61.9 | 58.6 |

[a] Sequence of TL modified DNA = CGACGT*TTGCAGC where * indicates position of the TL rather than a phosphodiester; [b] Sequence of DNA target = GCTGCAAACGTCG; [c] Sequence of RNA target = GCUGCAAACGUCG ; [d] melting temperatures ($T_m$s) were determined using 3 μM of each ON at pH 7.0 in 10 mM phosphate buffer containing 200 mM NaCl; $\Delta T_m$ = difference between modified ON and ON 5 (control).

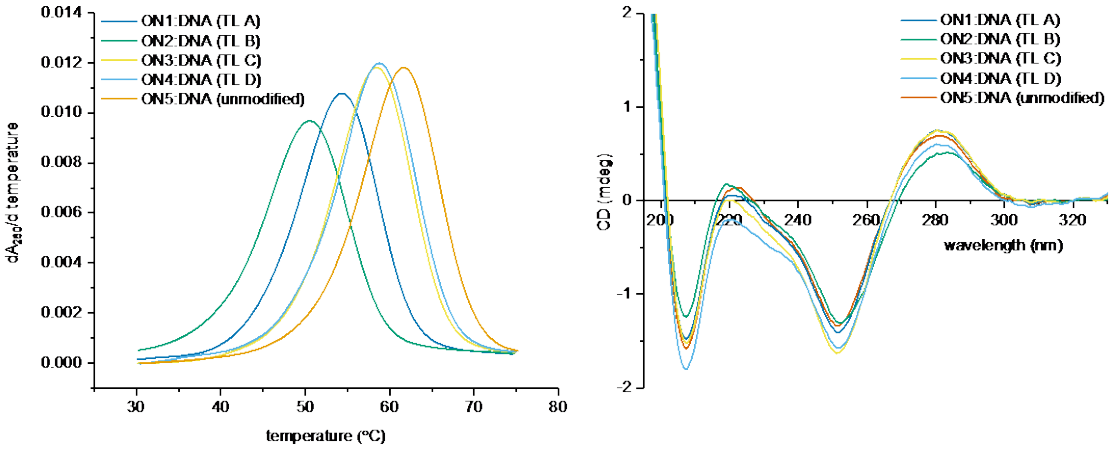


**Figure 4**. Left) UV melting studies of TL modified DNA:DNA duplexes (1st derivative of melting curve, Figure S2). Right) CD spectra of TL modified DNA:DNA duplexes. For sequences see Table 1.

Next, we compared the effect of the TLs on duplexes with complementary RNA (Figure 5). Again, the 5 bond 1,4 TL **B** was most destabilising ($\Delta T_m$ = -13.6 °C). In agreement with the literature,[37] the 7 bond 1,4 TL **A** was also significantly destabilising ($\Delta T_m$ = -5.3 °C). As with the DNA:DNA duplexes the 6 bond 1,4 TL **C** and 1,5 TL **D** linkages were least destabilising; however, when hybridised to RNA, the 1,4 TL **C** ($\Delta T_m$ = -0.8 °C) performed significantly better than the 1,5 TL **D** ($\Delta T_m$ = -3.3 °C).

Together, these results still suggest that 6 bonds is the optimum length for TLs in oligonucleotides, and also reveal that the previously reported 1,4 TL **C** is best at adopting the A-conformation required for DNA:RNA duplexes. This hypothesis is supported by CD, where all TL modified DNA:RNA duplexes adopt the A-conformation, but the duplex between ON 3 (TL **C**) and RNA overlaps best with the unmodified DNA:RNA spectrum (Figure 5).

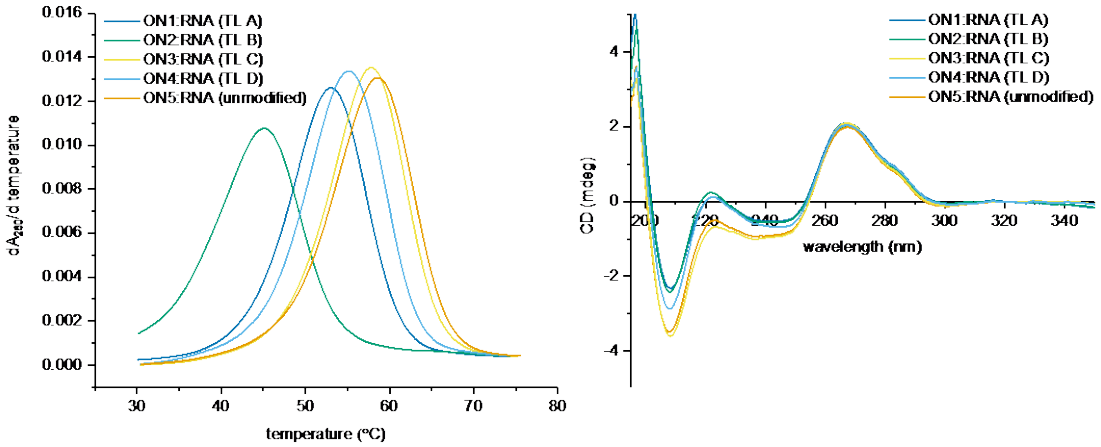


**Figure 5**. Left) UV melting studies of TL modified DNA:RNA duplexes (1st derivative of melting curve, Figure S2). Right) CD spectra of TL modified DNA:RNA duplexes. For sequences see Table 1.

## 2. Conclusions

Our results suggest that when developing a TL linkage for DNA or RNA-targeting applications the optimum number of chemical bonds between the sugars is 6, and a linkage that is one bond longer or shorter is detrimental to duplex stability. This is necessarily a somewhat simplistic conclusion as it is made in the absence of high-resolution NMR or crystallographic data for all the TL-linkages. The comparisons made in this study indicate that 1,4 TL **C**, originally developed by Florentiev, is a judicious choice for ASOs; it is only slightly destabilising in duplexes with a complementary RNA target, is charge neutral, and is stable to degradation by nucleases.[22] We anticipate that its use in combination with A-type ribose sugar analogues will further improve duplex stability. The 1,5 TL **D** should also be considered when choosing a triazole linkage for DNA-targeting applications, especially considering the simplicity of its synthesis relative to that of the similarly performing 1,4 TL **C**. Finally, given that aqueous conditions for preparing 1,5 triazoles have been reported for functionalization of carbohydrates and amino-acids,[38] we hypothesise that the 1,5 TL **D** may find applications in the nucleic acid field for gene synthesis. This is a subject of our ongoing investigations.

## 3. Experimental section

All reagents for synthesis were purchased from Sigma Aldrich and used without further purification. Standard DNA phosphoramidites, solid supports, and reagents were purchased from Link Technologies and Applied Biosystems. $CH_2Cl_2$ (over CaH) and pyridine (over KOH) were freshly distilled before use. Reactions were performed under an inert argon atmosphere in oven dried glassware. Reactions were monitored by thin-layer chromatography using Merck Kieselgel 60 F24 silica gel plates (0.22 mm thickness, aluminium backed), visualized by UV irradiation at 254/265 nm and by staining with *p*-anisaldehyde. Infrared (IR) spectra were recorded on a Bruker Tensor 27 FT-IR spectrometer fitted with an Attenuated Total Reflectance (ATR) sampling accessory. Absorption maxima are quoted in wavenumbers ($cm^{-1}$). $^1H$ and $^{13}C$ spectra were measured on a Bruker AVIII HD 400 spectrometer at 400 and 101 MHz, respectively. Chemical shifts are given in parts per million and were internally referenced to the appropriate residual solvent signal, all coupling constants (*J*) are quoted in Hertz (Hz). High-resolution mass spectra were measured on a Bruker 9.4 FT-ICR-MS mass spectrometer.

### *3.1. 5'-O-(4,4'-dimethoxytrityl)-thymidine-1,5 triazole-thymidine dimer (**3**)*

5'-O-(4,4'-dimethoxytrityl)-3'-O-propargylthymidine **1**[35] (0.64 g, 1.1 mmol) and 5'-azido-5'-deoxythymidine **2**[36] (0.182 g, 0.68 mmol) were dissolved in dioxane (10 mL). Cp*$RuCl(PPh_3)_2$ (0.11 g,

0.14 mmol) was added, followed by dioxane (5 mL) to ensure all reagents were in solution. The reaction was stirred under an argon atmosphere at 80 °C for 4 h. The solvent was removed *in vacuo* and the residue was dissolved in a $CH_2Cl_2$ (20 mL). This was washed with a 10% aqueous solution of EDTA (20 mL), a saturated aqueous solution of $NaHCO_3$ (20 mL), and water (20 mL). The organic phase was dried over $Na_2SO_4$ and the solvent removed *in vacuo* to give the crude product as a brown foam which was purified by flash chromatography (0-5% MeOH in EtOAc, where the column was pre-equilibrated using 0.5% pyridine in EtOAc). A second purification by flash chromatography (0-5% MeOH in $CH_2Cl_2$, where the column was pre-equilibrated using 0.5% pyridine in $CH_2Cl_2$) was required to give **3** as a pale yellow foam (0.55 g, 0.65 mmol, 95%).

$R_f$ (10% MeOH/$CH_2Cl_2$) 0.37; $n_{max}$ (FTIR) 1684, 1508, 1466, 1364, 1249, 1177, 1032 $cm^{-1}$; $d_H$ (400 MHz, $CDCl_3$) 10.30 (s, 1H), 9.86 (s, 1H), 7.52 (s, 1H), 7.51 (s, 1H), 7.33 – 7.12 (m, 9H), 6.81 – 6.73 (m, 4H), 6.67 (s, 1H), 6.28 (dd, *J* = 9.1, 5.2 Hz, 1H), 6.14 (t, *J* = 6.6 Hz, 1H), 4.73 (dd, *J* = 14.7, 4.1 Hz, 1H), 4.66 (dd, *J* = 14.7, 5.0 Hz, 1H), 4.57 – 4.42 (m, 4H), 4.27 (app q, *J* = 4.7 Hz, 1H), 4.12 (app d, *J* = 5.1 Hz, 1H), 4.08-4.06 (m, 1H), 3.71 (s, 6H), 3.43 (dd, *J* = 10.7, 3.2 Hz, 1H), 3.23 (dd, *J* = 10.7, 2.6 Hz, 1H), 2.50 (dd, *J* = 13.6, 5.2 Hz, 1H), 2.35 – 2.24 (m, 1H), 2.16 – 1.95 (m, 2H), 1.81 – 1.73 (m, 3H), 1.45 – 1.38 (m, 3H); $d_C$ (101 MHz, $CDCl_3$) 164.2, 164.1, 158.9, 151.6, 150.8, 144.3, 136.1, 135.3, 135.3, 134.0, 133.8, 130.2, 128.2, 128.2, 127.4, 113.5, 112.2, 111.7, 87.3, 85.5, 84.9, 84.1, 84.1, 81.0, 71.6, 63.9, 59.4, 55.4, 49.5, 39.0, 37.2, 12.5, 12.0; HRMS (ESI-TOF, MeOH): $M^-$, found 848.32557. $C_{44}H_{46}O_{11}N_7^-$ requires 848.32608.

*3.2. 5'-O-(4,4'-dimethoxytrityl)-thymidine-1,5 triazole-thymidine phosphoramidite (**4**)*

Nucleoside **3** (173 mg, 0.20 mmol) was dissolved in anhydrous degassed $CH_2Cl_2$ (5 mL). Degassed DIPEA (88 µL, 51 mmol) and 2-cyanoethyl *N*,*N*-diisopropylchlorophosphoramidite (68 µL, 0.30 mmol) were added and the reaction was stirred under an argon atmosphere at room temperature for 2 h. The reaction mixture was diluted with $CH_2Cl_2$ (20 mL) and washed with a saturated aqueous solution of KCl (30 mL). The organic phase was dried over $Na_2SO_4$ and the solvent evaporated *in vacuo* to give the crude product as a yellow oil, which was purified by flash chromatography (89:10:1 EtOAc:hexane:pyridine) to give the phosphoramidite **4** (155 mg, 0.15 mmol) as a white foam in 74% yield.

$R_f$ (89:10:1 EtOAc:hexane:pyridine) 0.31; $d_p$ (162 MHz, $CDCl_3$) 149.34, 149.03; HRMS (ESI-TOF, MeCN): $MH^+$, found 1050.44879.$C_{53}H_{65}N_9O_{12}P^+$ requires 1050.44848.

*3.3. Oligonucleotide synthesis*

Unmodified DNA and RNA were synthesized according to previously reported methods.[29] Modified oligonucleotides were synthesized using automated solid-phase oligonucleotide synthesis on 1.0 µmol scale involving cycles of acid-catalysed detritylation, coupling, capping, and iodine oxidation using an Applied Biosystems 394 synthesiser. Standard DNA phosphoramidites were coupled for 50 s, whereas extended coupling time of 10 min was used for the triazole dimer phosphoramidites. Coupling efficiencies were ≥98.0% in all cases as determined by the inbuilt automated trityl cation conductivity monitoring facility. Following removal of the 4,4'-dimethoxytrityl group, the oligonucleotides were cleaved from the solid support and the protecting groups were cleaved from the nucleobase and backbone by treatment with concentrated aqueous ammonium hydroxide for 60 min at room temperature followed by heating in a sealed tube for 5 h at 55 °C.

Once deprotected, the oligonucleotides were purified by reverse-phase high performance liquid chromatography (HPLC) on a Gilson system equipped with a Luna 10 µm C8(2) 100 Å pore Phenomenex column (250 × 10 $mm^2$) using a gradient of 10-20% acetonitrile in 0.1 M triethylammonium bicarbonate (TEAB) over 20 min with a flow rate of 4 mL/min. Elution was monitored by UV absorption between 260 nm and 295 nm.

*3.4. UV melting ($T_m$) analyses*

UV melting analysis was performed using a Cary 4000 Scan UV-Visible Spectrophotometer. 3 µM of each oligonucleotide was dissolved in 10 mM phosphate buffer containing 200 mM NaCl at pH 7.0 and denatured by heating to 85 °C (10 °C/min). The samples were then cooled to 20 °C and reheated to 85 °C at a rate of 1 °C/min, recording the absorbance of the sample at 260 nm as a function of temperature. This was repeated three times and the melting temperature calculated using in built software to determine the maxima of the 1$^{st}$ derivative of the melting curve. All UV melting studies were performed in duplicate with errors of less than $\pm$0.5 °C.

*3.5. CD spectroscopy*

Samples from the UV melting studies were then used to record the CD spectra for each TL modified DNA duplexed with DNA or RNA. CD spectra were recorded on a Chirascan Plus spectropolarimeter using quartz optical cells with a path length of 1.0 mm. The scans were performed at 25 °C in the region of 190-350 nm using a step size of 0.5 nm, a time per point of 1.0 s, and a bandwidth of 2 nm. Origin software was used to calculate the average of four scans and the traces were Savitzky-Golay-smoothed using a polynomial order of 2 and a smoothing window of 20 points. The resulting traces were baseline-corrected using the offset at 320 nm.

**Acknowledgments**

This work was supported by UK EPSRC Impact Acceleration Award grant EP/R511742/1 and UK BBSRC Grants BB/S018794/1 (New oligonucleotide analogues for therapeutic applications), BB/ J001694/2 (Extending the boundaries of nucleic acid chemistry), and BB/R008655/1 (New and versatile chemical approaches for the synthesis of mRNA and tRNA). We also thank ATDBio Ltd. for a studentship for A.T. and The National Science Centre (Poland, UMO-2018/28/T/ST5/00109) for a travel grant for P.W.

**References and notes**


1. Zamecnik, P.C. & Stephenson, M.L. Inhibition of Rous sarcoma virus replication and cell transformation by a specific oligodeoxynucleotide. *Proc. Natl. Acad. Sci. U. S. A.* **75**, 280-284 (1978).
2. Khvorova, A. & Watts, J.K. The chemical evolution of oligonucleotide therapies of clinical utility. *Nature Biotechnology* **35**, 238 (2017).
3. Moreno, P.M.D. & Pêgo, A.P. Therapeutic antisense oligonucleotides against cancer: hurdling to the clinic. *Frontiers in chemistry* **2**, 87-87 (2014).
4. Veltrop, M. & Aartsma-Rus, A. Antisense-mediated exon skipping: Taking advantage of a trick from Mother Nature to treat rare genetic diseases. *Experimental Cell Research* **325**, 50-55 (2014).
5. Sharma, V.K. & Watts, J.K. Oligonucleotide therapeutics: chemistry, delivery and clinical progress. *Future Med. Chem.* **7**, 2221-2242 (2015).
6. Sharma, V.K., Sharma, R.K. & Singh, S.K. Antisense oligonucleotides: modifications and clinical trials. *MedChemComm* **5**, 1454-1471 (2014).
7. Deleavey, G.F. & Damha, M J. Designing Chemically Modified Oligonucleotides for Targeted Gene Silencing. *Chem. Biol.* **19**, 937-954 (2012).
8. Khvorova, A. Oligonucleotide Therapeutics — A New Class of Cholesterol-Lowering Drugs. *N. Engl. J. Med.* **376**, 4-7 (2017).
9. Aartsma-Rus, A. & Krieg, A.M. FDA Approves Eteplirsen for Duchenne Muscular Dystrophy: The Next Chapter in the Eteplirsen Saga. *Nucleic Acid Ther.* **27**, 1-3 (2016).
10. Aartsma-Rus, A. FDA Approval of Nusinersen for Spinal Muscular Atrophy Makes 2016 the Year of Splice Modulating Oligonucleotides. *Nucleic Acid Ther.* **27**, 67-69 (2017).
11. Crooke, S.T. & Geary, R.S. Clinical pharmacological properties of mipomersen (Kynamro), a second generation antisense inhibitor of apolipoprotein B. *Br. J. Clin. Pharmacol.* **76**, 269-276 (2013).
12. Weng, Y., Xiao, H., Zhang, J., Liang, X.-J. & Huang, Y. RNAi therapeutic and its innovative biotechnological evolution. *Biotechnol. Adv.* **37**, 801-825 (2019).
13. Keam, S.J. Inotersen: First Global Approval. *Drugs* **78**, 1371-1376 (2018).
14. Geary, R.S., Norris, D., Yu, R. & Bennett, C.F. Pharmacokinetics, biodistribution and cell uptake of antisense oligonucleotides. *Adv. Drug Deliv. Rev.* **87**, 46-51 (2015).
15. Nuzzi, A., Massi, A. & Dondoni, A. Model Studies Toward the Synthesis of Thymidine Oligonucleotides with Triazole Internucleosidic Linkages Via Iterative Cu(I)-Promoted Azide–Alkyne Ligation Chemistry. *QSAR & Combinatorial Science* **26**, 1191-1199 (2007).
16. Madhuri, V. & Kumar, V.A. Design and Synthesis of Dephosphono DNA Analogues Containing 1,2,3-Triazole Linker and Their UV-Melting Studies with DNA/RNA. *Nucleosides, Nucleotides and Nucleic Acids* **31**, 97-111 (2012).
17. Varizhuk, A., Chizhov, A. & Florentiev, V. Synthesis and hybridization data of oligonucleotide analogs with triazole internucleotide linkages, potential antiviral and antitumor agents. *Bioorganic Chemistry* **39**, 127-131 (2011).
18. Lucas, R. et al. Microwave-assisted synthesis of a triazole-linked 3'–5' dithymidine using click chemistry. *Tetrahedron Letters* **49**, 1004-1007 (2008).

19. Sanzone, A.P., El-Sagheer, A.H., Brown, T. & Tavassoli, A. Assessing the biocompatibility of click-linked DNA in Escherichia coli. *Nucleic Acids Research* **40**, 10567-10575 (2012).
20. Birts, C.N. et al. Transcription of Click-Linked DNA in Human Cells. *Angewandte Chemie International Edition* **53**, 2362-2365 (2014).
21. Isobe, H., Fujino, T., Yamazaki, N., Guillot-Nieckowski, M. & Nakamura, E. Triazole-Linked Analogue of Deoxyribonucleic Acid (TLDNA): Design, Synthesis, and Double-Strand Formation with Natural DNA. *Organic Letters* **10**, 3729-3732 (2008).
22. Varizhuk, A.M. et al. Synthesis of Triazole-Linked Oligonucleotides with High Affinity to DNA Complements and an Analysis of Their Compatibility with Biosystems. *The Journal of Organic Chemistry* **78**, 5964-5969 (2013).
23. El-Sagheer, A.H. & Brown, T. Efficient RNA synthesis by in vitrotranscription of a triazole-modified DNA template. *Chemical Communications* **47**, 12057-12058 (2011).
24. Dallmann, A. et al. Structure and Dynamics of Triazole-Linked DNA: Biocompatibility Explained. *Chemistry – A European Journal* **17**, 14714-14717 (2011).
25. El-Sagheer, A.H. & Brown, T. Combined nucleobase and backbone modifications enhance DNA duplex stability and preserve biocompatibility. *Chemical Science* **5**, 253-259 (2014).
26. Varizhuk, A., Chizhov, A., Smirnov, I., Kaluzhny, D. & Florentiev, V. Triazole-Linked Oligonucleotides with Mixed-Base Sequences: Synthesis and Hybridization Properties. *European Journal of Organic Chemistry* **2012**, 2173-2179 (2012).
27. Kumar, P., Truong, L., Baker, Y.R., El-Sagheer, A.H. & Brown, T. Synthesis, Affinity for Complementary RNA and DNA, and Enzymatic Stability of Triazole-Linked Locked Nucleic Acids (t-LNAs). *ACS Omega* **3**, 6976-6987 (2018).
28. Sharma, V.K. et al. Synthesis and biological properties of triazole-linked locked nucleic acid. *Chemical Communications* **53**, 8906-8909 (2017).
29. Kumar, P., El-Sagheer, A.H., Truong, L. & Brown, T. Locked nucleic acid (LNA) enhances binding affinity of triazole-linked DNA towards RNA. *Chemical Communications* **53**, 8910-8913 (2017).
30. Zhang, L. et al. Ruthenium-Catalyzed Cycloaddition of Alkynes and Organic Azides. *Journal of the American Chemical Society* **127**, 15998-15999 (2005).
31. Johansson, J.R., Beke-Somfai, T., Said Stålsmeden, A. & Kann, N. Ruthenium-Catalyzed Azide Alkyne Cycloaddition Reaction: Scope, Mechanism, and Applications. *Chemical Reviews* **116**, 14726-14768 (2016).
32. Pedersen, D.S. & Abell, A. 1,2,3-Triazoles in Peptidomimetic Chemistry. *European Journal of Organic Chemistry* **2011**, 2399-2411 (2011).
33. von Matt, P. & Altmann, K.-H. Replacement of the phosphodiester linkage in oligonucleotides by heterocycles: the effect of triazole- and imidazole-modified backbones on DNA/RNA duplex stability. *Bioorganic & Medicinal Chemistry Letters* **7**, 1553-1556 (1997).
34. von Matt, P., Lochmann, T. & Altmann, K.-H. Replacement of the phosphodiester linkage in oligonucleotides by heterocycles: synthesis of thymidine dinucleotide analogs with triazole-modified backbones. *Bioorganic & Medicinal Chemistry Letters* **7**, 1549-1552 (1997).
35. El-Sagheer, A.H. & Brown, T. New strategy for the synthesis of chemically modified RNA constructs exemplified by hairpin and hammerhead ribozymes. *Proceedings of the National Academy of Sciences* **107**, 15329-15334 (2010).

36. Bannwarth, W. Solid-Phase Synthesis of Oligodeoxynucleotides containing phosphoramidate internucleotide linkages and their specific chemical cleavage. *Helvetica Chimica Acta* **71**, 1517-1527 (1988).
37. Palframan, M.J., Alharthy, R.D., Powalowska, P.K. & Hayes, C.J. Synthesis of triazole-linked morpholino oligonucleotides via CuI catalysed cycloaddition. *Organic & Biomolecular Chemistry* **14**, 3112-3119 (2016).
38. Kim, W.G. et al. Nickel-Catalyzed Azide–Alkyne Cycloaddition To Access 1,5-Disubstituted 1,2,3-Triazoles in Air and Water. *Journal of the American Chemical Society* **139**, 12121-12124 (2017).